ELSEVIER

International Journal of Pharmaceutics 238 (2002) 29–41

international journal of pharmaceutics

www.elsevier.com/locate/ijpharm

Dissolution kinetics of paracetamol single crystals

Korlakunte V.R. Prasad [1], Radoljub I. Ristic [2], David B. Sheen, John N. Sherwood *

Department of Pure and Applied Chemistry, University of Strathclyde, Glasgow G1 1XL, UK

Received 11 October 2001; received in revised form 1 February 2002; accepted 5 February 2002

Abstract

The dissolution anisotropy of paracetamol crystals grown in the presence and absence of the molecularly similar additive, *p*-acetoxyacetanilide (PAA) was studied under controlled conditions using a single crystal dissolution method in undersaturated aqueous solutions. Linear dissolution rates were determined for all the major habit faces by measuring their movement (regression) with time in a flow cell using a microscope. The rates of dissolution of particular faces of the pure material were distinctly different in crystals of different morphology grown at different supersaturations. The dissolution rates of {001} and {110} faces of crystals grown in the presence of PAA (6.02% w/w in solution) are higher than those of pure paracetamol. The results correlate with the distribution of strain in the crystal and support the concept that integral strain increases the solubility and hence the dissolution rate of the material. The mechanism of the dissolution process at the {001}, {20$\bar{1}$} and {110} faces was defined using optical microscopy and X-ray topography. At all undersaturations above 1% the dissolution studies yielded well developed, structurally oriented, etch pits on both {001} and {20$\bar{1}$} faces while on the {110} face rough shallow etch pits were observed. On all three faces, this etch-pitting was considerably more widespread than the dislocation content of the sector and probably reflects a 2-dimensional nucleation process rather than a dislocation controlled mechanism.

Keywords: Dissolution; Dislocations; Strain; X-ray topography; Paracetamol; *p*-Acetoxyacetanilide

1. Introduction

Knowledge of dissolution behaviour and of the factors affecting dissolution processes is crucial in the design, evaluation, control and therapeutic efficacy of solid dosage forms (Ansel et al., 1995). An understanding of the dissolution rates, dissolution mechanism, solubility and physical stability of crystalline forms of pharmaceutical solids is also important from the physiological availability point of view. As a consequence interest has

* Corresponding author. Tel.: +44-141-548-2797; fax: +44-141-548-4822.

E-mail address: j.n.sherwood@strath.ac.uk (J.N. Sherwood).

[1] Department of Engineering Science, PowderJect Centre for Gene Drug Delivery Research, 43 Banbury Road, University of Oxford, Oxford OX2 6PE, England, UK.

[2] Department of Chemical and Process Engineering, Firth Court, Western Bank, Sheffield University, Sheffield S1O 2TN, England, UK.

0378-5173/02/$ - see front matter © 2002 Published by Elsevier Science B.V.
PII: S0378-5173(02)00053-4

focused on the development of a reliable in-vitro dissolution test method that can characterise positively the in-vivo dissolution rate-controlled adsorption of drugs (Levy et al., 1965; Cohen et al., 1990).

Fundamental to the analysis of the results of such methods is the definition of the mechanism of the dissolution process and the factors that influence this. It is proposed that dissolution of a crystal face initiates and develops at surface regions within which a dislocation line emerges. Dislocations are thermodynamically unstable and form the core of a distorted region in the crystal lattice. The associated stress energy results in a localised increase in free energy and a reduction in the activation energy for dissolution at points where they emerge at the crystal surface (Burt and Mitchell, 1981; Chernov, 1989). Thus one could speculate that a crystal with higher dislocation density should have a higher thermodynamic activity which, in turn, may result in a greater overall dissolution rate when the process is under surface control. Dislocation associated strain is not, however, the only factor that could be responsible for the nucleation and development of the dissolution process. Other factors, such as impurity and solvent inclusion, mechanical deformation, crystal habit, surface energetics, and interaction between the solute and the solvent molecules could also have a major influence on the process (Garcia et al., 1999; Addadi et al., 1985; Burt and Mitchell, 1980; Fini et al., 1995). In the present paper we examine the influence of some of these factors on the dissolution characteristics of paracetamol single crystals.

Several researchers have reported on the dissolution behaviour of paracetamol either as single crystals (Chow et al., 1985; Shekunov and Grant, 1997; Shekunov et al., 1997) or on compacted discs (Chan and Grant, 1989). The initial stages of the dissolution of paracetamol single crystals in non-aqueous solutions was studied by Vasil'chenko et al. (1996). In this paper we report dissolution kinetic measurements carried out on all the major, accessible habit faces of pure and impurity doped paracetamol single crystals using a single crystal dissolution method. This method has the advantage that it allows the assessment of the average dissolution rate of the full crystal face and does not focus on localised contributions such as the regions around the emergence points of dislocation cores (Mullin and Garside, 1967; Burt and Mitchell, 1979; Shekunov and Grant, 1997; Shekunov et al., 1997). It also allows a better assessment to be made of the role of substructure in the overall process.

2. Materials and methods

2.1. Crystal growth

Single crystals (3–5 mm) of paracetamol were grown from commercially available material (Rhone Poulenc; Rhodapap) by controlled slow evaporation of a saturated solution in ethanol or water at 23 °C over a period of 3–4 weeks. The crystals were harvested and dried quickly using soft tissue paper. Crystals were of either columnar habit with major {110} faces or tablet-like with major {001} faces. The predominant faces for the columnar form in order of morphological importance were $\{110\} > \{001\} > \{20\bar{1}\} > \{011\}$ and for the tablet-like crystals, $\{001\} > \{110\} > \{011\} > \{20\bar{1}\} > \{100\}$ (Fig. 1). These habits correspond to those reported in the literature and

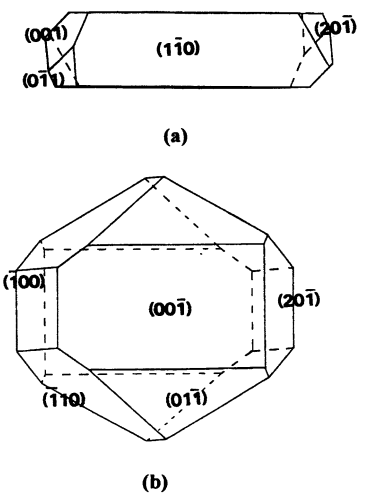

Fig. 1. Schematic morphologies of (a) columnar and (b) platelike crystals of paracetamol grown at low (< 5–7%) and high ($> 15\%$) supersaturations, respectively.

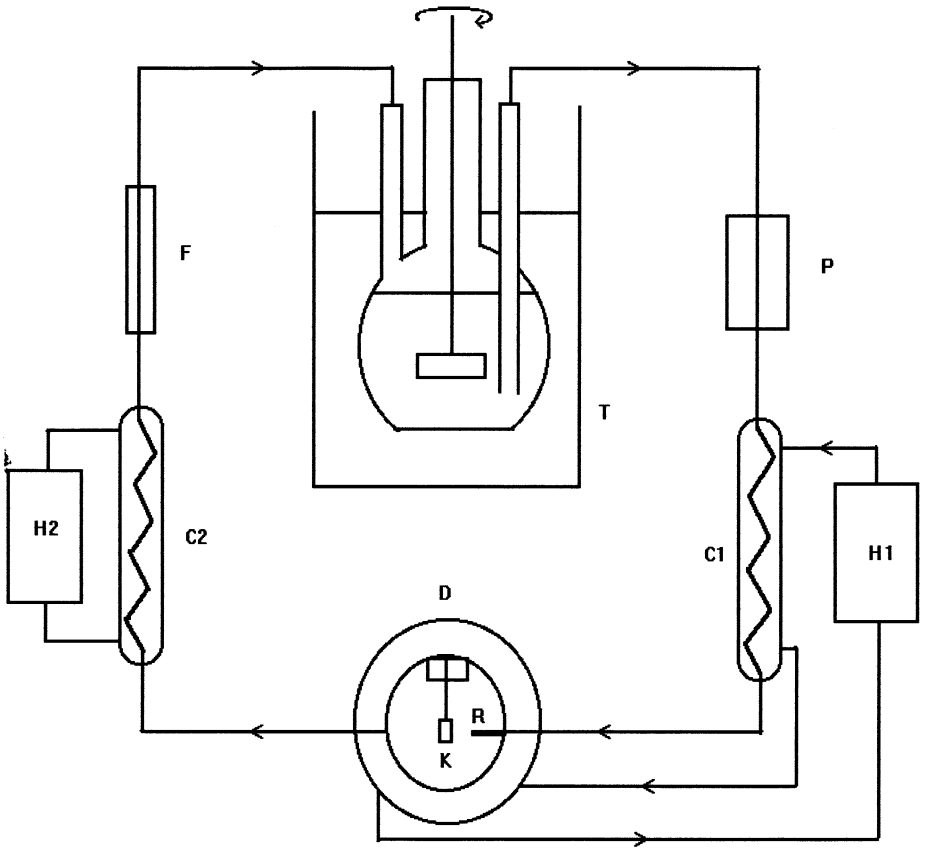

Fig. 2. Schematic diagram of the experimental equipment for the measurements of dissolution kinetics of paracetamol (T, thermostated water bath; P, pump; C1 and C2, heat exchangers; H1 and H2, Haake thermostated bath; D, dissolution cell; K, crystal; R, platinum resistor temperature probe; F, flow meter.

reflect growth under conditions of low ($S = 5$–7%) and high supersaturation ($S > 15\%$), respectively (Finnie et al., 1996; Ristic et al., 2001). Crystals selected for the dissolution experiment were 4–5 mm in size with well-defined habit faces. The PAA doped paracetamol crystals were grown at 23 °C from aqueous solution containing 6.02% w/w of PAA over a period of 3–4 weeks. The habit of these crystals was similar to that of the columnar form of the pure crystals except that the aspect ratio (a/c) was higher (Prasad et al., 2001a).

2.2. Dissolution studies

A schematic diagram of the experimental equipment used for the dissolution measurements is shown in Fig. 2. A saturated solution of paracetamol in water was prepared in a flat bottomed flask of capacity 2000 cm^3 at 25 °C and equilibrated in a thermostated water bath at the same temperature. The solution was continuously stirred at the rate of ~ 50 rpm. The solvent was pumped from the flask through heat exchanger-I to the water jacketed stainless steel cell (capacity 15 ml). The heat exchanger-I and the dissolution cell were maintained at the same temperature using pumped water from a thermostat H1 (Haake F6-C35). The solution was then returned to the reservoir through heat exchanger-II and a calibrated glass flow meter (Platon, range 50–800 $cm^3\ min^{-1}$). The temperature of the heat exchanger-II was maintained at the solution temperature (saturation temperature, 25 °C) using a

second thermostat bath, H2 Haake F3-CH). The temperature of the cell and the heat exchanger-I were raised above the saturation temperature in order to achieve the desired undersaturations. The cell temperature was monitored using a platinum resistance probe and indicator (Control techniques). The flow rate was maintained throughout the experiments at 600 cm^3 min^{-1}.

The crystal was glued to a stainless steel needle using a slow setting epoxy resin and mounted so that the face to be observed was normal to the direction the solution flow. The needle was then adjusted so that one edge of the crystal face to be observed coincided with the cross hair of the microscope eyepiece (Olympus CH, magnification $\times 40$) and the face itself was parallel to the direction of observation. The solution temperature was raised as quickly as possible to achieve the required undersaturation. The relative undersaturations ($S = \ln(C_w/C_s)$, where C_w is the solubility at the working temperature and C_s is the solubility at the saturation temperature) were determined from the solubility data of Grant et al. (1984).

As the crystal dissolved, the regression of the face was measured as a function of time using a micrometer eyepiece (± 0.1 μm). Dissolution measurements were stopped once the crystal face started 'rounding off'. This effect signalled the preferential dissolution of the edges and corners of the face. For each undersaturation level, the linear dissolution rate, R, was obtained from the gradient of a plot of horizontal displacement of the edge (face) versus dissolution time. The flow rate of the solution (~ 600 cm^3 min^{-1}), was shown from preliminary experiments to be high enough to prevent diffusion control of the dissolution process. Satisfactory measurements could be made on the {001} and {110} faces of the columnar crystals of the pure and PAA doped material. The other end faces were too small for accurate examination. For the plate-like crystals an assessment could also be made of the {100}, {0$\bar{1}$1} and {20$\bar{1}$} faces.

2.3. X-ray topography

X-ray transmission topography (Lang, 1973; Klapper, 1980) was used to investigate the distribution in the crystals of structural defects such as dislocations, lattice strain and inclusions and to correlate these (particularly dislocations) with the dissolution behaviour.

Oriented sections were cut from grown crystals using a solvent saw. The sections were polished to a thickness of ~ 1 mm using water soaked tissue placed on a flat glass surface before being used for the X-ray topographic analysis. All topographs were recorded on Agfa structurix D4 X-ray film using Cu K_α radiation. Slices cut parallel to {001} and {010} faces were used and topographs recorded using the diffraction vectors $\boldsymbol{g}$, 110 and $\boldsymbol{g}$, 002.

3. Results

3.1. Dissolution curves

Fig. 3 shows a typical series of plots of the horizontal displacement of the crystal edge of the {20$\bar{1}$} habit face as a function of dissolution time at different undersaturation levels. These were linear for all faces examined showing that the dissolution rate, R, was constant and independent of time, whilst the face remained flat.

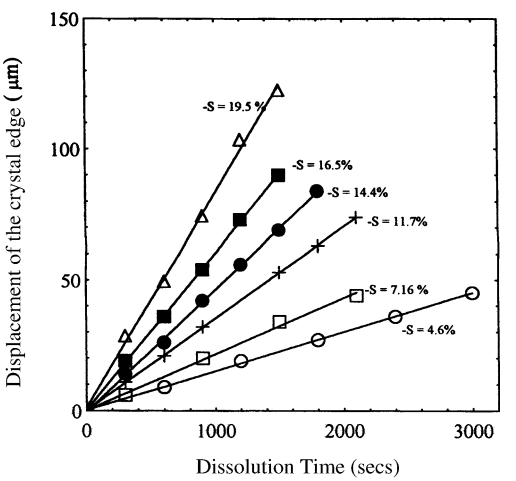

Fig. 3. Horizontal displacement of the edge of the {20$\bar{1}$} habit face of a paracetamol crystal as a function of dissolution time at different undersaturation levels.

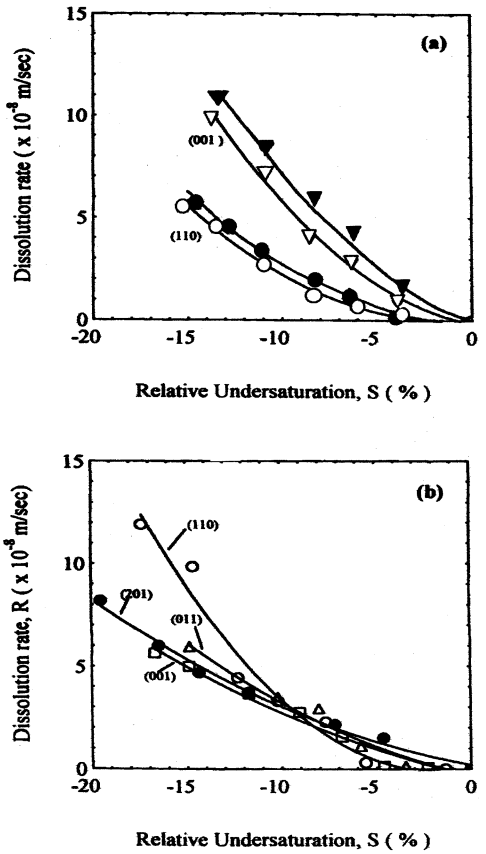

Fig. 4. Variation of the dissolution rates of the faces of pure paracetamol crystals as a function of relative undersaturation for (a) columnar and (b) plate-like crystals of paracetamol. The open points on 4(a) refer to the dissolution rates of the pure crystals and the full points to PAA doped crystals. All points on 4b refer to pure crystals.

The linear dissolution rates measured as a function of undersaturation for all accessible habit faces of both columnar and plate-like crystals of pure paracetamol are shown in Fig. 4a and b, respectively. Also shown in Fig. 4a for easier comparison are the dissolution rates of the equivalent faces of the PAA doped columnar crystal. The dissolution behaviour was found to be a non-linear function of undersaturation for all growth sectors examined.The short period of time available for measurement before the faces commenced 'rounding off', coupled with the need to maximise the accuracy of the dissolution measurement, meant that only one crystal face could be used at each supersaturation in each experiment. The results expressed thus represent the behaviour of a total of 5–6 separate crystals in each experiment (*circa* 50 in the total study) and thus represent a broad survey of the range of crystals available. This procedure was, in itself, a time consuming process. To repeat each point for a sufficient number of times to allow a statistical analysis would have been prohibitive. Sufficient checks were carried out, however, to show that variation in dissolution rate of one face from crystal to crystal prepared in the same manner was less than 5%.

Comparison of the two sets of curves in Fig. 4a show a similar relationship between the dissolution rates of the {001} and {110} faces of both types of specimen. The former shows a distinctly faster dissolution rate than the latter. The rates of dissolution of the doped crystals are marginally higher than those of the pure crystals over the full range of undersaturation. In contrast, there are significant differences between the dissolution rates of these faces on the columnar and plate-like pure crystals.

Despite the fact that etch-pitting can be induced to occur at the emergent ends of dislocation cores (Finnie et al., 2001), the dissolution rates for both the {110} and {001} faces of the plate-like crystals, at low undersaturations ($< 5\%$) are immeasurably small. As the undersaturation is increased, the dissolution rates of both faces increase non-linearly with that of the {110} now exceeding the dissolution rate of the {001} face. This divergence continued to the maximum possible undersaturation achievable (20%). The remaining faces that are large enough in these plate-like specimens to be studied show a regular variation that parallels that of the {001} face. There are only small variations in behaviour between the {001}, $\{20\bar{1}\}$ and {100} faces. In contrast, the difference in behaviour between the {110} and {001} faces in the two types of crystal is quite distinctive; the relative rates of dissolution of these faces being reversed between the two crystal types. This demonstrates well that different types of crystal of the same material prepared under different conditions can show quite different dissolution behaviour.

The overall results and their variation are considerably different to those published by Shekunov and Grant (1997) and Shekunov et al. (1997) for the dissolution of the surfaces of crystals of undefined history using the optical interferometry technique. The difference probably reflects not only the lack of differentiation of the crystals used into columnar or tabular forms but also the difference in experimental approach. The present method assesses the average dissolution rate of all active centres across the face whereas the interferometry method focuses on specific dissolution centres such as dislocation sources and follows each separately for short periods of time. Such techniques are useful for defining the specific properties of such sources. We believe, however, that the present method represents more accurately the dissolution characteristics of the average crystal surface and forms a better link to the eventual end use of the data obtained.

3.2. Surface microscopy

The surfaces of the dissolved crystals showed little variation in topography over the range of undersaturations studied. Even at the very lowest undersaturation ($\sim 1\%$) all surfaces showed a high degree of surface etch-pitting (Fig. 5). On the {001}, {20$\bar{1}$} and {001} surfaces, the pits were geometrically oriented with respect to the underlying crystal lattice being elongated, quadrangular shaped on {001} and pyramidally shaped on {20$\bar{1}$}. The pits were sharp and distinct and were similar in reverse to the growth hillock shapes identified previously on the same surfaces Ristic et al. (2001) and to dislocation etch-pits produced under much lower conditions of undersaturation (Vasil'chenko et al., 1996; Finnie et al., 2001).

In contrast, the etch pits produced on {110} surfaces of pure crystals were rounded, shallow and less distinct. Better shaped pits resulted on

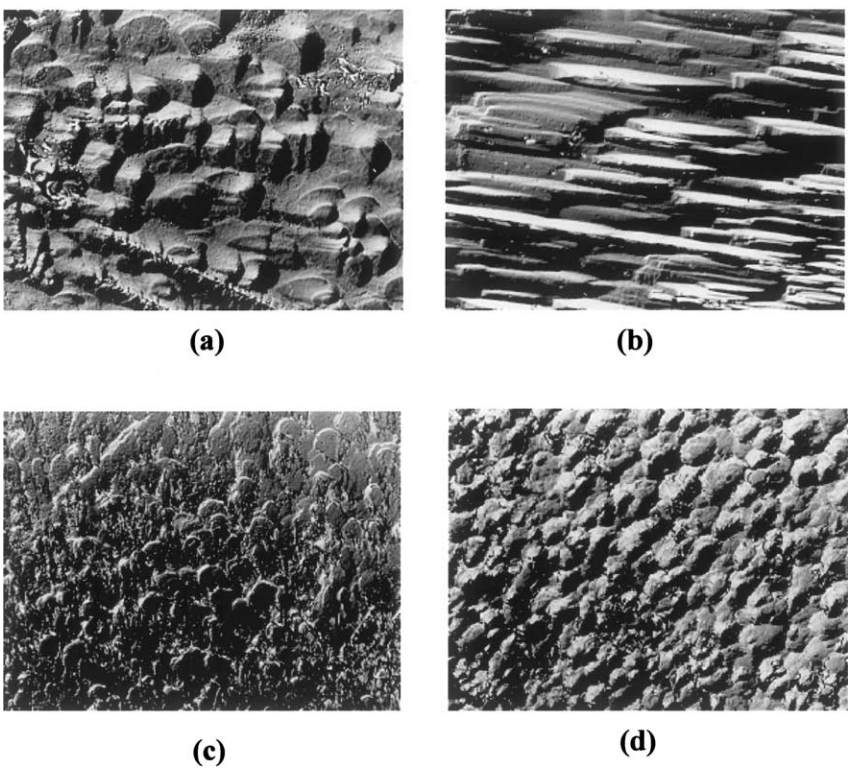

Fig. 5. Dissolution etch patterns on the (a) {20$\bar{1}$}, (b) {001} (c) {110} faces of pure paracetamol crystals. (d) The {110} face of a paracetamol crystal doped with 6.02% PAA (all micrographs 500 ×).

the {110} surfaces of the PAA doped crystals but these were still less distinct than on other faces. The density of etch pits could be evaluated as {110}, 3×10^5 cm^{-2}; {001}, 1×10^5 cm^{-2}; {20$\bar{1}$}, 4×10^5 cm^{-2} and {110} doped, 4×10^5 cm^{-2}. There was no observable change in etch-pit density with increasing undersaturation over the full range studied but the pits on all faces became increasingly diffuse.

3.3. X-ray topography

X-ray topography shows the distribution of strain and defects in the underlying growth sectors of the crystal (Klapper 1980; Halfpenny et al., 1997). In order to demonstrate general distinctions between the sectors we present typical examples of sections of columnar, pure crystals (Fig. 6a and b), plate-like pure crystals (Fig. 6c and d) and columnar PAA doped crystals (Fig. 6e and f).

In the columnar crystals grown at low supersaturations the dominant faces grow by a dislocation nucleated birth and spread mechanism-{110} and a screw dislocation mechanism-{001} (Ristic et al., 2001). The growth steps associated with the hillocks, which propagate, by the latter mechanism are rough which potentially allows solvent incorporation into the developing face and sector. Fig. 6a shows a (010), longitudinal, section of a columnar crystal. This defines well the existence of high strain along the core of the crystal and which emerges at the {001} and {20$\bar{1}$} faces at the ends of the crystal. In comparison the two {110} growth sectors which meet at the {100} edges are much more perfect. The quality of the latter is better defined in the {001}, transverse, section (Fig. 6b) which allows the resolution of the peripheral {110} sectors. The central core (dominantly the {001} and {20$\bar{1}$} sectors) of this section can again be seen to be defective but the peripheral {110} sectors contain well defined dislocation images threading through relatively perfect lattice to the bounding surfaces.

Fig. 6c and d, which present equivalent views of a crystal grown at high supersaturations, show a completely different defect structure. Under these conditions of growth, the growth mechanism of the {110} sectors changes from a dislocation controlled mechanism to one in which growth occurs by the propagation of large macrosteps which nucleate at the corners and edges of the face (Ristic et al., 2001). The consequence is that solvent inclusions are trapped in the developing lattice. This gives rise to the darkly contrasted (highly strained) volumes in the {110} sectors (Fig. 6d) together with white volumes which are so very highly strained that they fail to diffract the X-rays at all. In contrast the remaining sectors are much more perfect than both the {110} sectors of this type of crystal and the equivalent core sectors in Fig. 6a. This increased perfection is defined in the {010} section shown in Fig. 6c. This now shows no core disorder in the {001} and {20$\bar{1}$} sectors. Instead, well-defined dislocation bundles radiate from the nucleation point to all of the bounding facets in this plane. The remaining lattice is relatively perfect.

Addition of the additive PAA to the crystallising solution inhibits growth, particularly of the {110} sectors (Hendricksen et al., 1998; Prasad et al., 2001a). High supersaturations are, therefore, required to develop the crystal. Under these circumstances, the crystals develop morphologically in much the same manner as do the pure crystals at low supersaturation. The major distinction is that the impurity predominantly contaminates the {110} surfaces and sectors. The molecule of PAA is 1.24 times larger in volume than the paracetamol molecule (Finnie et al., 1999). It is not surprising then that its incorporation causes a straining of the lattice through both the size difference and the associated disruption of the hydrogen bonding network. In such a brittle material (Finnie et al., 2001; Prasad et al., 2001b), such strain will be retained and not released by plastic deformation. This is confirmed by the topograph shown in Fig. 6e and f. The peripheral {110} sectors are dark and narrow resulting from included strain and restricted growth, respectively. The central portions show a similar but possibly increased strain compared with that in Fig. 6b but this is much less marked than the former difference.

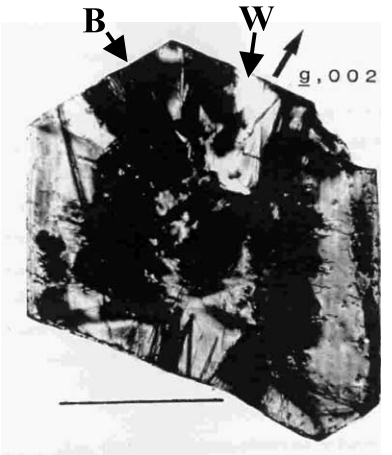
B
W
g,002

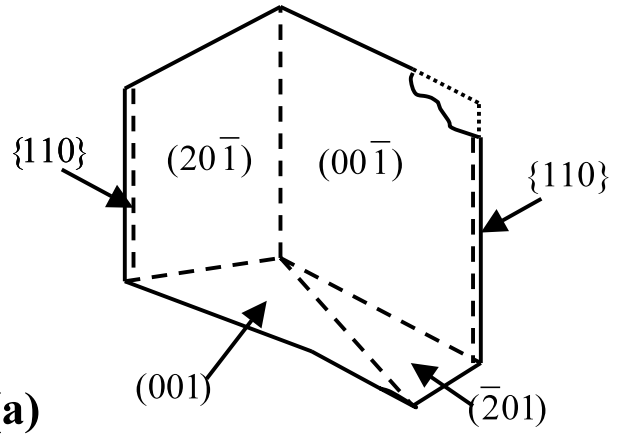
{110}
(20$\bar{1}$)
(00$\bar{1}$)
{110}
(001)
($\bar{2}$01)

(a)

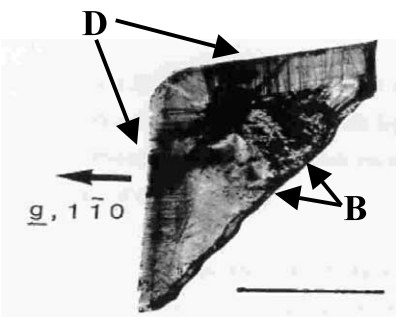
D
g,1$\bar{1}$0
B

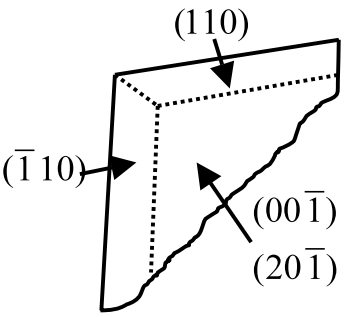
(110)
($\bar{1}$10)
(00$\bar{1}$)
(20$\bar{1}$)

(b)

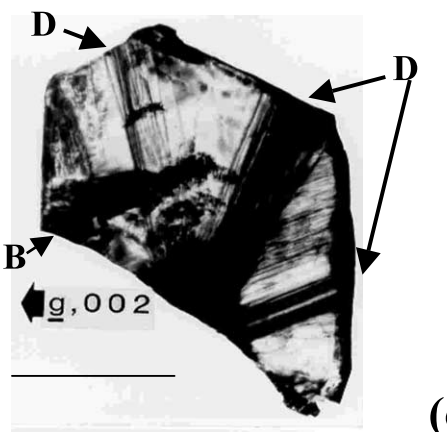
D
D
B
g,002

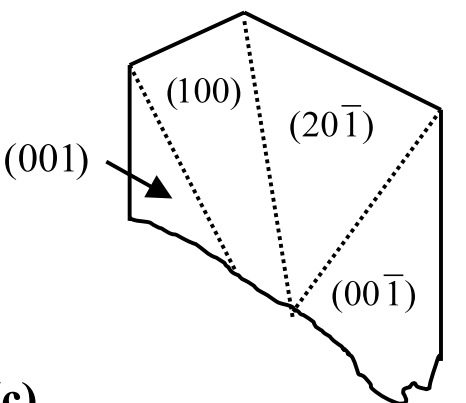
(100)
(20$\bar{1}$)
(001)
(00$\bar{1}$)

(c)

Fig. 6.

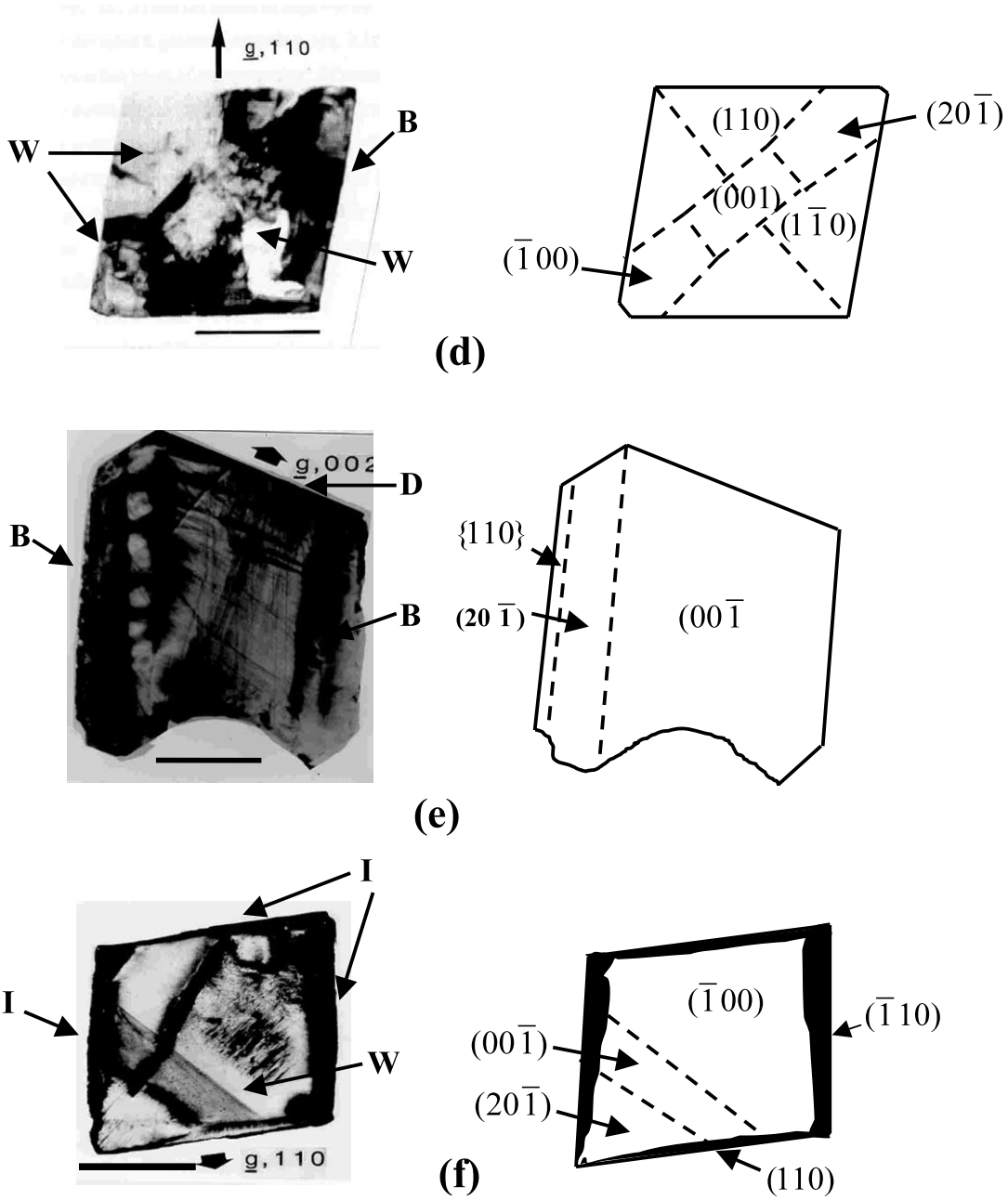

Fig. 6. (*Continued*)

4. Discussion

Theories of dissolution regard the process as the reverse of crystal growth. Thus at the simplest, it might be assumed, as it is for growth, that the relative dissolution rates of the different crystal faces would follow the order of their surface attachment energies (Hartman and Bennema,

1980). Such an assumption implies that dissolution and growth are dominantly thermodynamically controlled processes and that kinetic factors are less influential. This may be true in some cases but is by no means generally so. This dilemma has particular relevance in the case of paracetamol. Calculation and comparison of the attachment energies for potential faces yields relative growth rates for each face ($R \sim E_{att}$) and hence morphologies for paracetamol (Ristic et al., 2001). Although this approach predicts many of the basic growth forms of the crystal it yields a different morphology to either of those observed in practice. Thus mechanistic factors must dominate in the growth process.

Using values of the attachment energy calculated using a DREIDING II intermolecular potential (Ristic et al., 2001) and relating the results to the reverse process of dissolution would suggest an order of dissolution rate; $\{100\} = \{001\} > \{20\bar{1}\} = \{011\} = \{010\} > \{110\} > \{111\} > \{021\}$.

This does not reflect the order of the dissolution rates observed. Obviously mechanistic factors dominate in dissolution as they do in the growth of this material. In both processes the mechanisms are believed to be controlled by the defect structure of the crystal surface and the underlying crystal lattice.

Most theories of dissolution regard the initiating defects to be the emergent ends of dislocations at the crystal face. The strain which develops around the dislocation core defines a higher free energy in these regions of the surface compared with the remainder and hence a greater ease of nucleation for both growth and dissolution. (Chernov, 1989). That such processes do occur at very low undersaturation is well defined, and indeed the method is used to detect the emergent ends of growth dislocations at surfaces (Thomas and Williams, 1971; Halfpenny et al., 1984). Dislocation etching alone occurs, however, only at very low undersaturations ($\ll 1\%$) and then often only in the presence of a dissolution inhibitor (Vasil'chenko et al., 1996; Prasad et al., 2001a; Gilman and Johnstone, 1962). The more general pattern of etching which develops as the undersaturation is increased still follows the underlying structure of the surface but is much more widespread than both the number of dislocations present and their location. The distinction can be seen by comparing the etch patterns on Fig. 5 with the topographs of Fig. 6. The former show dissolution etch patterns comprising $\sim 10^5$–10^6 etch pits cm^{-2} whilst the latter shows few (in some cases no) dislocations in some of the corresponding sectors (Fig. 6d) or much lower numbers, e.g. Fig. 6 b, 10^3 dislocations cm^{-2}. Additionally, the dissolution etch patterns are widespread across the crystal face whereas, in the main, growth dislocations are isolated in groups around a line normal to the face and which develops from the nucleation point (Fig. 6c).

From this evidence we propose that the influence of growth dislocations on the dissolution process is minor at undersaturations in the range 1% and upward and dominates only at very low undersaturations to yield very low dissolution rates. Whereas dislocations will continue to function with increasing undersaturation, this mechanism becomes overtaken by a process of

Fig. 6. X-ray topographs of thin sections of crystals of paracetamol grown under different conditions showing the variation in strain content that develops on growth under differing conditions of supersaturation and purity. In general, relatively perfect lattice reproduces as a grey contrast. Extended strain appears as either volumes of black contrast (B) or, if giving a high distortion, white (W). Dislocations (D) are readily recognisable as black lines, usually radiating from the nucleus or from points of inclusions to the bounding surfaces. I indicates impurity induced strain. The accompanying diagrams show the distribution of the growth sectors intersected by the crystal sections and allow a judgement of the sectoral distribution of the strain which underlies the surfaces examined, (a) Columnar crystal grown at low supersaturation (< 5–7%) (010) section. (scale mark 3.5 mm). (b) Columnar crystal grown at low supersaturation (< 5–7%), (001) section. (scale mark 2.5 mm). (c) Plate-like crystal grown at high supersaturation ($> 15\%$), (010) section. (scale mark 2 mm). (d) Plate-like crystal grown at high supersaturation ($> 15\%$), (001) section. (scale mark 2.5 mm). (e) Columnar crystal grown at high supersaturation ($\sim 20\%$) in the presence of 6.04% w/w *p*-acetoxyacetanilide, (010) section. (scale mark 2 mm). (f) Columnar crystal grown at high supersaturation ($\sim 20\%$) in the presence of 6.04% w/w *p*-acetoxyacetanilide, (001) section. (scale mark 2.5 mm)

two-dimensional nucleation, which occurs at suitably energetic sites at the crystal surface. This will initiate at some critical undersaturation, which will be defined by the nature of the site, the structure underlying the surface and solvent interaction with the sites and the surface. From this point, dissolution will accelerate at a rate controlled, not now by the number of nucleation sites, which are numerous, $\sim 10^6$ cm^{-2}, but by the defect nature of the underlying structure. Thus we would expect to see the observed behaviour; zero to low dissolution rates at very low undersaturations (dislocation control) giving way to accelerating dissolution with increasing undersaturation (2d nucleation control). This behaviour will vary slightly from face to face of the crystal depending on the crystallographic nature of the face and possibly the degree of interaction of the solvent with the face. This then provides the basic anisotropy of dissolution and for relatively perfect sectors the variation will not be large. Further variations will then be introduced by differences in the defect nature of the underlying structure of each face. These will be caused by processing variations that lead to differences in growth mechanism and consequently in impurity incorporation, inclusion formation, mechanical deformation and the general lattice strain that these entities cause. This situation will be characteristic of the dissolution processes of most drug materials in vivo where medium to high supersaturation conditions will hold for the dissolution process.

The dominant influence of lattice strain is well exemplified by the variations in dissolution rate noted for the present material.

As noted above, processing variations lead to both significant changes in growth mechanism and sub-structure. The latter has the controlling influence on the rate of dissolution. Comparison of Fig. 4a and b in conjunction with the topographic evidence provides the basis for this conclusion.

In these figures, the dissolution rates for {001} and {110} faces differ considerably between the two sample types, reversing the order of dissolution rate between the samples. If the overall basis for the process were simply the nucleation rate at the surface coupled with the crystal structure of the underlying sector, then we would accept some minor variations between the crystals, but not the noted reversal. Other major differences in the nature of the dissolving sector must have an influence. The topography supplies the evidence. As Fig. 6a shows, the {110} sectors show relatively perfect lattice threaded by small numbers of isolated dislocations. There is some variation in lattice strain as evidenced by the growth banding parallel to the {110} faces. In general, however, the sector would be regarded as highly perfect. This situation is typical for this sector in crystals prepared in this fashion (low supersaturation $<$ 5%). In such a crystal we see (Fig. 4a) that the rate of dissolution of this face follows the average pattern for the dissolution of all faces (cf. Fig. 4b) of 'good' perfection. On the other hand, the {001} face which bounds a highly strained sector (Fig. 6a), shows a considerably higher dissolution rate. A different mode of processing (growth at high supersaturation $>15\%$) yields {001} sectors of high perfection (Fig. 6b) which show the average dissolution rate characteristic of such faces (Fig. 6b). In contrast, the same mode of processing leads to the development of considerable strain from solution inclusion in the {110} sectors (Fig. 6b and c) and a much higher dissolution rate for this sector. This reversal in dissolution rates for these two sectors between the two samples can thus be attributed to the difference in strain between the sectors.

Fig. 6c summarises the influence of impurities on both the crystal lattice and its dissolution rate. The presence of the molecularly similar impurity inhibits growth and results in impurity incorporation. To produce even slow growth requires high supersaturations but the product is a columnar crystal since the impurity restricts the growth of the {110} face to a much greater extent than the {001} face. The defect structure of the resulting crystal is similar to that of the pure columnar crystals but with the added problem that the incorporated impurity causes strain within the host lattice. This is well exemplified by the dark volumes at the {110} edges of the topograph (Fig. 6 e and f) which define this incorporation. The overall result is that the observation of the same

order of dissolution rate for the {110} and {001} faces as for the pure columnar crystals with each being slightly enhanced by the presence of impurity included strain.

Finally, it is worth confirming that the parallel variations in strain and inclusion content to those noted here occur also in small crystals produced by bulk crystallisation (Prasad et al., 2001a). Thus the conclusions made here for observations on large crystals (mm dimensions) should carry over to commercial materials (10–100 μm dimensions).

5. Conclusions

Dissolution of paracetamol crystals at undersaturations greater than a fraction of 1% takes place by a 2-dimensional nucleation and spread mechanism which when established becomes dominantly controlled by the strain developed in the lattice through processing variations and by impurity inclusion. These variations can lead to significant differences in dissolution rates between samples derived from different sources and prepared under different conditions. The provocation of such variations by changes in processing conditions or purity could lead to the engineering of samples with controlled dissolution properties and hence to the control of dosage forms and drug behaviour.

Acknowledgements

The authors gratefully acknowledge the financial support of this work by the UK EPSRC and the three pharmaceutical companies Pfizer, Roche and SmithKline Beecham. It was carried out under a programme entitled 'Particle Formation, Processing and Characterisation for the Pharmaceutical Industry' involving the Universities of Bradford, Strathclyde and Surrey. They also thank the Director and staff of the Rutherford Appleton Daresbury Laboratory for the provision of facilities for the X-ray experiments.

Appendix A. Nomenclature

(hkl)	single crystallographic plane or crystal face
$\{hkl\}$	family of crystallographic planes or crystal faces
$[hkl]$	specific crystallographic direction
C_w	concentration at working temperature
C_s	concentration at saturation temperature
R	dissolution rate
S	supersaturation (+) or undersaturation (−)

References

Addadi, L., Berkovitch-Yellin, Z., Weissbuch, I., van Mil, J., Shimon, L.J.W., Lahav, M., Leiserowitz, L., 1985. Growth and dissolution of organic crystals in the presence of additives—a contribution to stereochemistry and materials science. Angew. Chemie. 97, 476–496.

Ansel, H.C., Popovich, N.G., Allen, L.V., 1995. Pharmaceutical Solid Dosage Forms and Drug Delivery Systems, 6th ed. Williams & Wilkins Publishers, London.

Burt, H.M., Mitchell, A.G., 1979. Dissolution anisotropy in nickel sulfate α hexahydrate crystals. Int. J. Pharm. 3, 261–274.

Burt, H.M., Mitchell, A.G., 1980. Effect of habit modification on dissolution rate. Int. J. Pharm. 5, 239–251.

Burt, H.M., Mitchell, A.G., 1981. Crystal defects and dissolution. Int. J. Pharm. 9, 137–152.

Chan, H.K., Grant, D.J.W., 1989. Influence of compaction on the intrinsic dissolution rate of modified acetaminophen and adipic acid crystals. Int. J. Pharm. 57, 117–124.

Chernov, A.A., 1989. Formation of Crystals in Solutions. Contemporary Phys. 30, 251–276.

Chow, A.H.L. Chow, P.K.K., Zongshan, K.W.Z., Grant, D.J.W., 1985. Modification of acetaminophen crystals: influence of growth in aqueous solutions containing *p*-acetoxyacetanilide on crystal properties. Int. J. Pharm. 24, 239–258.

Cohen, J.L., Hubert, B.B., Leeson, L.J., Rhodes, C.T., Robinson, J.R., Roseman, T.J., Shefter, E., 1990. The development of USP dissolution and drug release standards. Pharm. Res. 10, 983–987.

Fini, A., Fazio, G., Fernandez-Hervas, M.J., Holgado, M.A., Rabasco, A.M., 1995. Influence of crystallisation solvent and dissolution behaviour for a diclofenac salt. Int. J. Pharm. 121, 19–26.

Finnie, S., Ristic, R.I., Sherwood, J.N., Zikic, A.M., 1996. Characterisation of growth behaviour of small paracetamol crystals grown from pure solutions. Chemical Engineering Research & Design (Trans. IChemE) 74A, 835–838.

Finnie, S., Kennedy, A., Prasad, K.V.R., Ristic, R.I., Sheen, D.B., Sherwood, J.N., 1999. *p*-Acetoxyacetanilide. Acta Crystallogr. C55, 234–236.

Finnie, S., Prasad, K.V.R., Sheen, D.B., Sherwood, J.N., 2001. Microhardness and dislocation identification studies on paracetamol single crystals. Pharm. Res. 18, 674–681.

Garcia, E., Veesler, S., Boistelle, R., Hoff, C., 1999. Crystallization and dissolution of pharmaceutical compounds-An experimental approach. J. Cryst. Growth 199, 1360–1364.

Gilman, J.J., Johnstone, W.G., 1962. Dislocations in LiF crystals. Solid State Physics 13, 147–222.

Grant, D.J.W., Medizadeh, M., Chow, A.H.I., Fairbrother, J.E., 1984. Non-linear van t'Hoff solubility temperature plots and their pharmaceutical interpretation. Int. J. Pharm. 18, 25–38.

Halfpenny, P.J., Roberts, K.J., Sherwood, J.N., 1984. Dislocations in Energetic Materials 4. Etching and Microhardness Studies of Pentaerythritol tetranitrate and Cyclotrimethylenetrinitrammine. J. Cryst. Growth 69, 73–81.

Halfpenny, P.J., Sherwood, J.N., Simpson, G.S., 1997. X-ray Topographic Studies of Organic and Non-linear Optical Materials. Il Nuovo Cimento 19, 123–135.

Hartman, P., Bennema, P., 1980. The attachment energy as a habit controlling factor. J. Cryst. Growth 49, 145–154.

Hendricksen, B.A., Grant, D.J.W., Meenan, P., Green, D.A., 1998. Crystallisation of paracetamol (acetaminophen) in the presence of structurally related substances. J. Cryst. Growth 183, 629–640.

Klapper, H., 1980. Defects in non-metal crystals. In: Tanner, B.K., Bowen, D.K. (Eds.), Characterisation of Crystal Growth Defects by X-ray Methods. Plenum Press, NY, USA, pp. 133–160.

Lang, A.R., 1973. The properties and observation of dislocations. In: Hartmann, P. (Ed.), Crystal Growth, an Introduction. North Holland, Amsterdam, pp. 444–492.

Levy, G., Leonards, J., Procknal, J., 1965. Development of in-vitro tests which correlate quantitatively with dissolution rate-limited drug absorption in man. J. Pharm. Sci. 54, 1719–1722.

Mullin, J.W., Garside, J., 1967. The crystallisation of aluminium potassium sulphate: A study in the assessment of crystallizer design data, Part I: Single crystal growth rates. Trans. Instn. Chem. Eng. 45, T285–T290.

Prasad, K.V.R., Ristic, R.I., Sheen, D.B., Sherwood, J.N., 2001a. Crystallisation of paracetamol from solution in the presence and absence of impurity. Int. J. Pharm. 215, 29–44.

Prasad, K.V.R., Sheen, D.B., Sherwood, J.N., 2001b. Fracture property studies of paracetamol single crystals using microindentation techniques. Pharm. Res. 18, 867–872.

Ristic, R.I., Finnie, S., Sheen, D.B., Sherwood, J.N., 2001. Macro and micro-morphology of monoclinic Crystals of paracetamol grown from pure aqueous solution. J. Phys. Chem. B105, 9057–9066.

Shekunov, B.Yu., Grant, D.J.W., 1997. In-situ optical interferometric studies of the growth and dissolution behaviour of paracetamol (acetaminophen). 1. Growth kinetics. J. Phys. Chem. B101, 3973–3979.

Shekunov, B.Yu., Grant, D.J.W., Latham, R.J., Sherwood, J.N., 1997. In-situ optical interferometric studies of the growth and dissolution behaviour of paracetamol (acetaminophen). 3. Influence of growth in the presence of *p*-acetoxyacetanilide. J. Phys. Chem. B101, 9107–9112.

Thomas, J.M., Williams, J.O., 1971. Dislocations and the Chemical Reactivity of Organic Solids. Solid State Chemistry 6, 119–154.

Vasil'chenko, M.A., Shakhtshneider, T.P., Naumov, D.Y.u., Boldyrev, V.V., 1996. Topochemistry of the initial stages of the dissolution of single crystals of acetaminophen. J. Pharm. Sci. 85, 929–934.